Werk

Jahr: 1981
Kollektion: fid.geo
Signatur: 8 Z NAT 2148:49
Digitalisiert: Niedersächsische Staats- und Universitätsbibliothek Göttingen
Werk Id: PPN1015067948_0049
PURL: http://resolver.sub.uni-goettingen.de/purl?PPN1015067948_0049

LOG Id: LOG_0035
LOG Titel: Simultaneous observation of an intense 65 keV field-aligned proton beam and ULF-waves during a break-up event
LOG Typ: article

Übergeordnetes Werk

Werk Id: PPN1015067948
PURL: http://resolver.sub.uni-goettingen.de/purl?PPN1015067948
OPAC: http://opac.sub.uni-goettingen.de/DB=1/PPN?PPN=1015067948

Contact

Niedersächsische Staats- und Universitätsbibliothek Göttingen
Georg-August-Universität Göttingen
Platz der Göttinger Sieben 1
37073 Göttingen
Germany
Email: gdz@sub.uni-goettingen.de

J Geophys (1981) 49:123–127

Journal of Geophysics

Simultaneous Observation of an Intense 65 keV Field-Aligned Proton Beam and ULF-Waves During a Break-up Event

W. Stüdemann and C.K. Goertz

Max-Planck-Institut für Aeronomie, D-3411 Katlenburg-Lindau 3, Federal Republic of Germany

Abstract. Measurements of nearly mono-energetic 65 keV protons above active auroral forms were obtained on a rocket flight from Andenes (Norway) on 13 October 1977. Analysis of the pitch angle distribution of the >30 keV protons and the azimuthal anisotropy of the proton fluxes support a model of a proton beam of finite spatial extent. The particle observations occur simultaneously with ULF-waves in the frequency range 0.5–5 Hz. The particle distribution function is unstable and causes an amplification of obliquely propagating Alfvén waves. We argue that the waves are amplified by resonant interaction with the proton beam.

Key words: Particle acceleration – Monoenergetic ions – ULF waves – Wave-particle interaction – Break-up phase – Magnetospheric substorm

Introduction

The energization of plasmas occuring over auroral arcs is of great current interest and importance. This region is known to display the characteristic signatures of field-aligned acceleration of charged particles, which comprise an important part of the auroral current system. The mechanism of acceleration is still controversial simply because there are not enough measurements available to permit us to assess the role of any of the suggested mechanisms in a quantitative fashion. It is now believed that acceleration takes place at altitudes in the range ~1–3 earth radii (R_E), i.e., in regions not covered by rocket campaigns (Shawhan et al. 1978). Measurements made from rockets can detect (cheaply) the signatures of such acceleration mechanisms and thus provide crucial information for assessing the importance of particle energization.

In this note we report an especially spectacular case of ion acceleration which occured during a substorm on 13 October 1977 near auroral arcs. The case reported here is unusual in at least two ways. Firstly, the ions were found to be accelerated downwards along the magnetic field and secondly, the energy of the accelerated ions was of the order of 65 keV.

It has become customary to associate field aligned charged particle beams with acceleration by electrostatic fields parallel to the magnetic field. Such fields may exist along wirth others in double layers or regions of anomalous resistivity. However, the case reported here of field aligned 65 keV ions cannot be explained by electrostatic fields because electrons were not affected, quite apart from the rather extreme value of 65 kV for a field-aligned electrostatic potential. Neither can other mechanisms such as enhanced particle precicipation by pitch angle scattering, ion-cyclotron heating or betatron acceleration across field lines explain the observations.

In addition to its spectactular nature and rather puzzling features the event is characterised by a close temporal association of the ion beam with large amplitude ULF waves. The waves are most likely to be Alfvén waves confined to a narrow region in space. Such waves are in fact "kinetic Alfvén waves" (Hasegawa 1977) which can interact reasonantly with charged particles. We believe that our measurements are the first evidence from space for such a resonant interaction. Our understanding of this process is far from complete. Nevertheless, the process is significant and may play an important role in the magnetosphere-ionosphere coupling (Goertz and Boswell 1979).

Instrumentation

Basically, the instrument consists of a solid-state detector measuring electrons and a solid-state detector telescope for ions with charge $Z \geqq 1$, using a permanent magnetic field to separate the electrons and the ions. Details of the instrument and the calibration procedures are described elsewhere (Stüdemann and Winterhoff in press 1980). The energy ranges covered are 15–200 keV for electrons and 20–300 keV for protons. The energy resolution was set to 8 keV for the 7 lower energy channels and increased logarithmically above 80 keV. The system resolution of the detector-amplifier combination was 7 keV full width at half maximum. The geometric factors for isotropic particle fluxes are $2 \cdot 10^{-4}$ cm^2 sr for electrons and $5 \cdot 10^{-4}$ cm^2 sr for protons.

The data presented in this paper are taken from two identical sensor systems which measure at a pitch angle of about 20° and in the range 60°–100° due to built-in angles of 5° and 80° with respect to the rocket's spin axis and a nominal attitude of 20° between the spin axis and the geomagnetic field direction. The attitude was actively controlled by means of a gyro-based attitude control system and the actual pitch angle for each measurement was derived from the on-board magnetometer.

Observations

The payload F3A was launched on 13 October 1977 during a magnetospheric substorm which commenced at 20:22 UT and continued in several stages until 23:30 UT The substorm occurred during a period of low-level geomagnetic disturbance with Kp = 3−. During the substorm the disturbance in the X-com-

0340-062X/81/0049/0123/$01.00

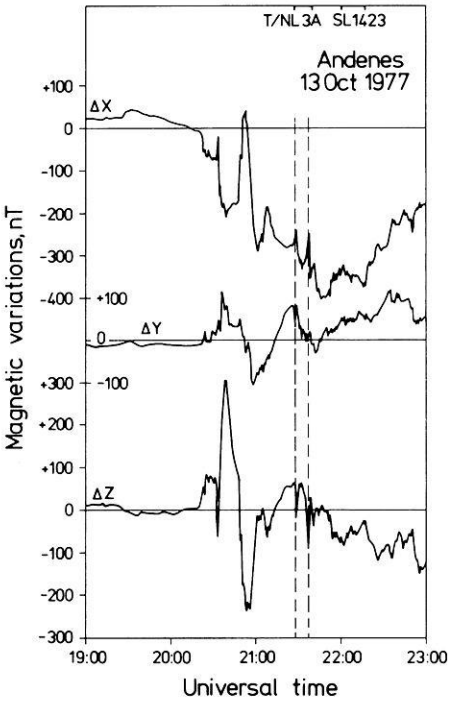

Fig. 1. Magnetometer recording at Andenes. The *dashed lines* mark the flight time of the payload F3A

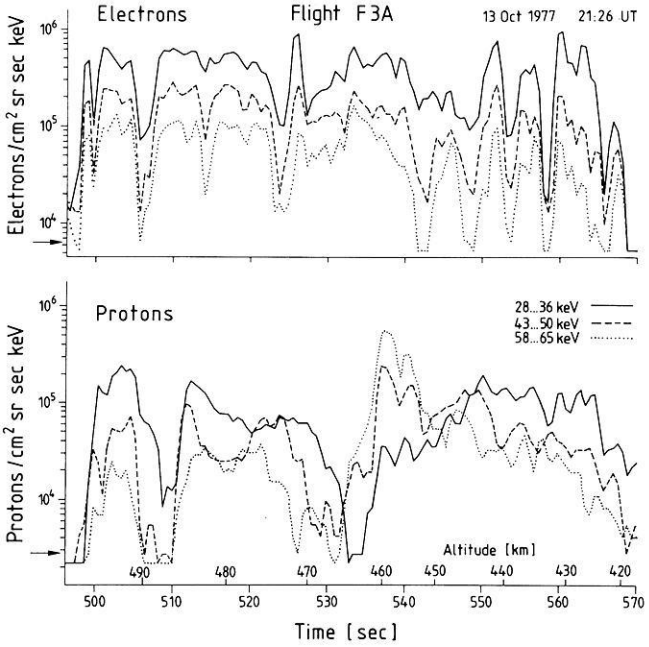

Fig. 2. Measurements of electron fluxes (*upper part*) and proton fluxes (*lower part*) at various energies for particles having pitch angles of about 20°. The *arrows* on the vertical axis mark the fluxes equivalent to one count per sampling interval. Energy passbands specified are the same for electrons and protons

ponent reached a maximum of 400 nT. Figure 1 is a magnetometer recording taken at the launch site in Andenes, Norway (McIllwain parameter $L=6.2$). Prior to the flight of F3A auroral activity was concentrated in a faint homogeneous arc with a sharp northern edge moving slowly to the south. The rocket was launched at 21:26 UT simultaneously with an intensification of the arc, a further decrease in the X-component and an increase in the micropulsation activity. During the first part of the flight the rocket crossed the bright arc with a maximum intensity of 50 kR in the 5,577 Å oxygen line approximately 120 s after launch. It reached the sharp northern edge at about 240 s flight time. At about 21:31 UT (300 s after launch) auroral break-up took place with rapid expansion of the aurora to the north.

The observations discussed in this paper were taken in the time interval 490–570 s flight time when the rocket was magnetically above a region of active discrete auroral luminosity of more than 20 kR for the 5,577 Å oxygen line. Figure 2 presents the measured electron and proton fluxes at different energies for this time interval. The data are taken from the sensor system which is directed nearly parallel to the rocket's spin axis and accepts particles having pitch angles around 20°. The arrows on the vertical axis mark a count rate of 1 count per sampling interval (0.1 s). The energy spectra of the protons normally follow a power law. Following the increase of the count-rates at about 534 s (altitude 460 km) the energy spectrum shows a well pronounced maximum near 65 keV energy. After 542 s the spectral curve starts to return to its original power law form. Figure 3 displays the peaked energy spectra for both sensors. The vertical bars represent the statistical uncertainties and the horizontal bars give the width of the energy passbands.

In Figure 4 the nature of the mono-energetic peak is investigated further by combining the measurements from two additional proton instruments on the same payload (courtesy of Schmidtke and Urban). The left-hand side of Fig. 4 is an exam-

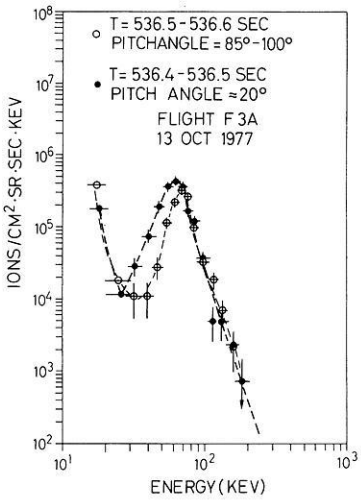

Fig. 3. Example out of a series of peaked ion energy spectra during flight F3A with data from two 100 ms sampling intervals. The energy axis of all ion measurements in this paper refers to the energy deposited in the sensitive volume of the solid state detector. In the case of protons a small correction term of a few keV must be added due to the energy loss in the dead layer of the solid state detector (>15 μg/cm², Al-contact)

ple of the normal power-law energy spectrum well before the observation of the mono-energetic peak. Nearly the same spectrum is again measured after the event at about 550 s. The measurements shown on the right-hand side of Fig. 4 are taken at the time when the peak was most pronounced. All measurements contained in Fig. 4 cover the pitch angle range 85°–100°. The figure demonstrates that all instruments agree very well where their energy ranges overlap giving high confidence to the

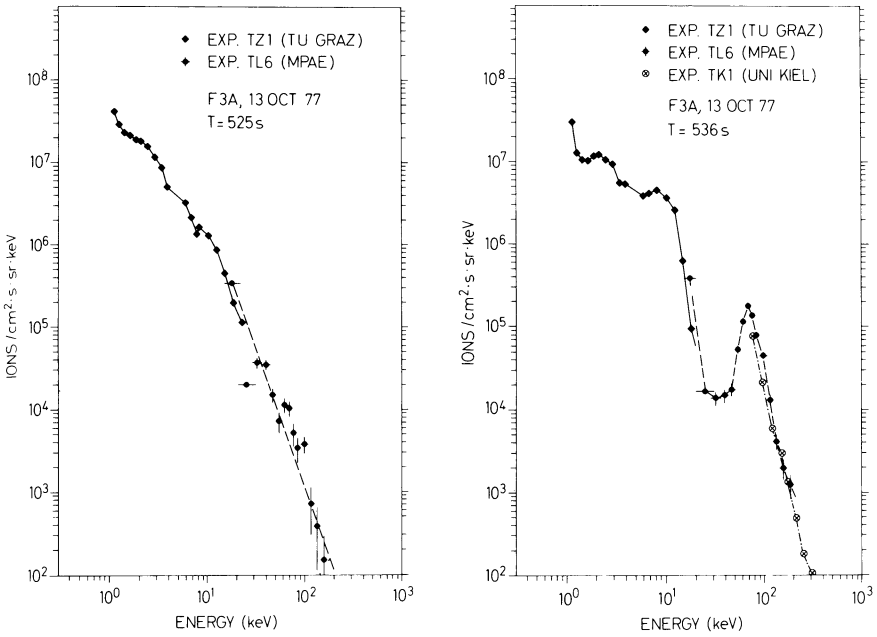

Fig. 4. Composition of energy spectra of all instruments sensitive to positive ions on the same rocket flight prior to the observation of the energy peak (*left side*) and during the event (*right side*). (Courtesy of Urban, University Graz, and Schmidtke, University Kiel)

observation of the mono-energetic proton peak. At the same time the pitch angle distributions measured for protons above 30 keV energy change from a normal distribution to a field-aligned pitch angle distribution. This transition can be seen in Fig. 5. Each panel contains data for half a spin rotation from both sensor systems. Fluxes at pitch angles above $\approx 70°$ stay nearly constant whereas the flux of precipitated protons increases.

Even at the highest time resolution of the spectral proton data we cannot detect any velocity dispersion in the data during the time interval 535–545 s. In contrast, such dispersion is clearly visible at the end of the previous burst (527–532 s, Fig. 2). We condude that the intensity variations following 532 s either originate from modulations in a region close to the point of observation or are the effect of spatial gradients in particle densitites. The first alternative seems unlikely because the electrons are not dramatically affected at this time, thus precluding any process involving static electric fields. The existence of a gradient in the proton density is supported by their azimuthal anisotropy. In Fig. 6 the upper curves represent the count-rates of the 80° sensor (60°–100° pitch angle) at times when the sensor is looking eastward (crosses) and westward (dots) at the same pitch angle of 80°. From these curves an anisotropy factor A is calculated defined as the ratio between the difference in fluxes seen from the east and the west and the sum of both (Fig. 6, upper middle part). This anisotropy could be caused either by $E \times B$-drift (E is electric field, B magnetic) or by density gradients. Using measured values for the perpendicular electric field of ~ 100 mV/m (Grabowsky, private communication) and the magnetic field of ~ 40.000 nT the $E \times B$ drift velocity is of the order of 1 km/s and far too small to account for the observed azimuthal anisotropy. Thus the anisotropy is interpreted as beeing due to a density gradient in the north-south direction (higher fluxes in the south, $A > 0$). The curves in the lower middle part of Fig. 6 show the flux of the precipitating proton beam with the highest time resolution obtainable for reference. During the steep increase at 536 s and, even more pronounced, during the decreases following 538 s and 541 s A becomes large. Our interpretation is as follows: The north-going rocket is overtaken

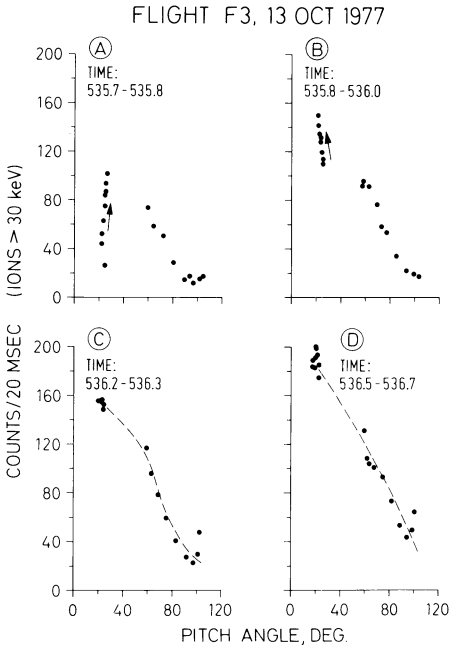

Fig. 5. Pitch angle distribution of protons above 30 keV showing the transition from a normal distribution prior to 535 s to a well pronounced field-aligned distribution. For further details see text

by a northwardly expanding region of higher proton precipitation at ≈ 536 s. As soon as its northern edge reaches the position of the rocket the anisotropy factor A drops to zero and becomes slightly negative. At this time the rocket is inside the region of enhanced proton precipitation with some indication that the tendency for A to become negative is caused by the approach to the southern edge of this narrow region. Thus the north-south extension, d, of the region is estimated to be of the order of 5 km. The northward movement slows down at 538 s and the rocket again leaves the region of high proton precipitation through its northern boundary (A positive again).

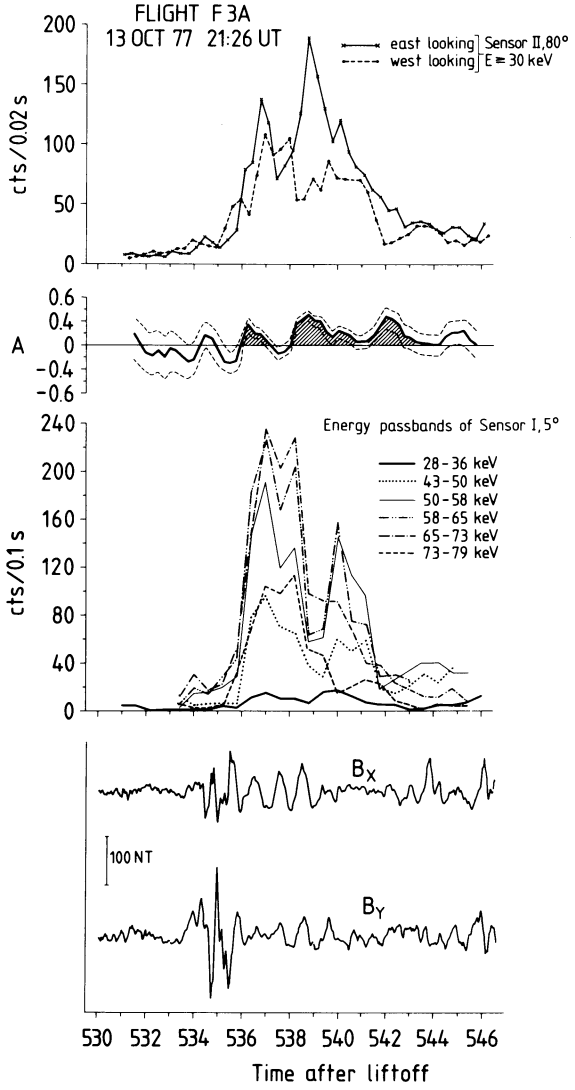

Fig. 6. Comparison between proton data with highest time resolution (0.02 s) available and measurements from the magnetometer (taken from Klöcker and Theile 1979, Fig. 2) for the time of observation of the peaked energy spectrum. Upper part: count-rates of the nearly perpendicular directed sensor in two azimuthal directions 180° apart for 80° pitch angle particles. *Upper middle part:* anisotropy factor A (defined in text) derived from the above curves. *Lower middle part:* count-rates of precipitated protons for different energies. *Lower part:* magnetic field variations (B_x = north, B_y = east components of the earth's magnetic field vector) after high pass filtering with a cut-off at 0.65 Hz

From these observations we deduce that the rocket enters, for a short time, a narrow region in which a mono-energetic proton beam of 65 keV with a field-aligned pitch angle distribution exists. The width of this region is estimated to be of the order of a few km. During the time when the rocket is close to or stays in this region the magnetometer detects ULF waves with a frequency of a few Hz and an amplitude of ≈ 100 nT (Klöcker and Theile 1979). For comparsion the B_x and B_y components of the magnetic field are reproduced in the lower part of Fig. 6.

Discussion

The remarkable temporal (and by implication spatial) association of the field aligned-ion beam and the ULF wave activity

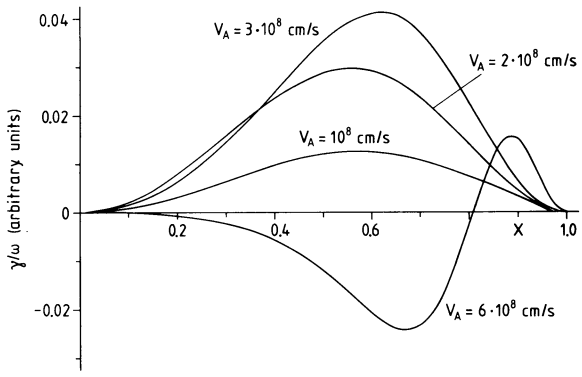

Fig. 7. Calculated growth rates, γ/ω, as a function of $x=(\omega/\omega_0)\cdot\tan\Theta$ for different values of the Alfvén velocity V_A according to the equation given in the text. The velocity V of the protons in the beam are taken to be equivalent to 65 keV, the thermal width V_0 of the beam is taken to be equivalent to 10 keV. For $V_A = 3\cdot 10^8$ cm/s the Alfvén velocity is about equal to the particle velocity

suggests a physical connection between the two in the sense that either the waves produce the beam (by non-linear trapping) or that the beam produces the waves (by amplification). The energy flux in the beam $P_b = 8.2$ erg/cm$^2\cdot$s is about equal to the energy flux in the waves. P_w:

$$P_w = \frac{b^2}{8\pi} V_g \simeq \frac{b^2}{8\pi} V_A = 11.9 \text{ erg/cm}^2\cdot\text{s}$$

b = perturbation of magn. field

where we have assumed that the group velocity of the ULF waves (V_g) is of the order of the Alfvén speed (V_A). Thus from an energetics point of view it is not clear which way the energy is flowing: from particles to waves or vice-versa. However, the ion-distribution function shows a well defined peak at 65 keV (not only the flux) and it is quite unlikely that such a distribution can be produced by particle trapping. On the other hand such a distribution is unstable and could give rise to a growth of obliquely propagating Alfvén waves (Fejer and Kan 1968). The resonant growth rate γ of a wave with frequency $f=\omega/2\pi$ and wave vector $\mathbf{k}=(k_\parallel, k_\perp)$ for an ion-beam of velocity $V = v V_A$ along the magnetic field and thermal width $V_0 = v_0 V_A$ is given by Fejer and Kan as

$$\gamma/\omega = -\pi^{1/2}\frac{m_e}{m_i}\frac{N_b}{N_o} X^2(1-X^2)((1-X^2)^{1/2}-v)\exp\left|-\left(\frac{(1-X^2)^{1/2}-v}{v_0}\right)\right|$$

where m_e and m_i are the electron and ion masses, $X = \omega\tan\Theta/\omega_0$, $\tan\Theta = k_\perp/k_\parallel$, N_b is the density of the beam and N_o is the background plasma density. $\omega_0 = (\Omega_i\Omega_e)^{1/2}$ is the lower hybrid frequency. This relation holds for a cold plasma (electron thermal velocity less than the Alfvén velocity). In Fig. 7 we show the calculated growth rates as a function of X for different values of V_A. We do not know the exact value of the Alfvén velocity because the average ion mass is not known. The measured plasma density at the rocket is 2×10^4 cm^{-3}. For a hydrogen plasma V_A is 6,800 km/s, and for an average ion mass of four atomic masses V_A is 3,400 km/s. We see that generally the maximum growth rate occurs at $X \approx 0.6$. Since locally $\omega_0 = 9\cdot 10^4$ Hz a frequency of 2 Hz is only appreciably amplified for nearly perpendicular propagation ($\tan\Theta \gg 1$). Furthermore the path length for the wave-particle interaction must be long

enough because the growth rates are small due to a ratio $N_b/N_o \approx 10^{-4}$. However, the waves may have been amplified further up the field line where ω_0 is less and N_b/N_o is larger. Nevertheless, an infinitely extended beam (perpendicular to the magnetic field) will in general amplify higher frequencies than are observed.

Waves which do not propagate in the finite sized beam for long enough, i.e., waves not guided exactly along the field, will be amplified less along their ray-path even though the local amplification rate in the beam could be larger. As we have argued above, the beam has a finite width ($d \simeq 5$ km). This finite width is of great importance because the approximate effective half width of the spatial Fourier spectrum of waves generated in the beam is

$$k_x \simeq 1/2d$$

and only waves with frequencies below ω_c will be effectively guided along the field lines, where ω_c is given by Fejer and Lee (1967)

$$\omega_c = \Omega_i \frac{1}{2} \left(\frac{m_e}{m_i}\right)^{1/2} \frac{c}{\omega_{pi} d}$$

$$\omega_{pi}^2 = \frac{4\pi N_0 e^2}{m_i}$$

$$\Omega_i = \frac{eB}{m_i c},$$

e = elementary charge,
$m_{e,i}$ = electron, ion mass,
B = magn. flux density,
c = speed of light.

Higher frequency waves are not confined to the narrow ion beam and, although the local growth rate may be larger, the waves will not stay in the beam long enough to be amplified to detectable levels. Using appropriate values for $d \approx 5$ km, $N_0 \approx 2 \cdot 10^4$ cm^{-3}, $m_i \approx 4\, m_{\text{proton}}$ and $B = 0.44$ G, we find

$$\omega_c \approx 4 \text{ Hz}.$$

Thus inside the beam we expect the frequency spectrum to show a peak near ω_c. Waves above ω_c should be observed outside the beam presumably at a reduced intensity. Waves below ω_c are confined to the beam but are amplified less. This is in excellent agreement with the ULF observations reported by Klöcker and Theile (1979).

It is interesting to note that at the time of observation of the magnetic ULF waves the electric field instrument on board the rocket measured large fluctuations of the electric field perpendicular to the earth's magnetic field. The amplitude of these fluctuations was of the order of 100 mV/m (Grabowsky, private communication) and the amplitude of the magnetic fluctuations are in accordance with the existence of an Alfvén wave.

The question of the ultimate origin of the beam has not been answered. We can rule out a number of possibilities without being able to suggest a reasonable explanation. Since the electrons do not show a decrease of intensity simultaneously with the increase of ions, electrostatic fields parallel to the magnetic field cannot be responsible for the ion beam. Enhanced pitch angle scattering into the loss-cone by ion-cyclotron waves in the magnetosphere would not cause the highly field-aligned beam observed. Betatron acceleration or ion-cyclotron heating would increase the perpendicular energy and a field-aligned beam would not be expected. The only, albeit highly speculative, suggestion we can make involves kinetic Alfvén waves (Hasegawa and Chen 1976; Hasegawa 1977), which at large distances along the field lines may have accelerated the ions up to the Alfvén speed. Kinetic Alfvén waves can be produced by drift wave instabilities and by mode conversion of shear Alfvén waves at steep gradients of plasma density, say at the plasmapause (Hasegawa and Chen 1976). Such an acceleration would be the inverse process of the one we have discussed above.

Acknowledgements. The authors wish to acknowledge the assistance of H.P. Winterhoff in manufacturing and calibrating the energetic particle instrument. For many fruitful discussions one of us (W.S.) wishes to thank Dr. K. Wilhelm. Measurements from additional instruments of the same payload were kindly provided by Dr. R. Grabowsky, W. Ott, and H. Wolf, APW, Freiburg; G.L. Schmidtke, University of Kiel; A. Urban, TU Graz; N. Klöcker, TU Braunschweig.

The rocket programme "Substormphenomena" was funded by the "Bundesministerium für Forschung und Technologie" and managed by the DFVLR-BPT.

References

Fejer, J.A., Kan, J.R.: A guiding centre Vlasov equation and its application to Alfvén waves. J. Plasma Physics, **3**, 331–351, 1969

Fejer, J.A., Lee, K.F.: Guided propagation of Alfvén waves in the magnetosphere. J. Plasma Phys. **1**, 387–406, 1967

Goertz, C.K., Boswell, R.W.: Magnetosphere-ionosphere coupling. J. Geophys. Res. **84**, 7239, 1979

Hasegawa, A.: Kinetic properties of Alfvén waves. Proc. Indian Acad. Sci. **86**, 151, 1977

Hasegawa, A., Chen, L.: Kinetic processes in plasma heating by resonant mode conversion of Alfvén wave. Phys. Fluids **19**, 1924, 1976

Klöcker, N., Theile, B.: Magnetic ULF-waves in the vicinity of active auroral forms. J. Geophys. **46**, 229–236, 1979

Shawhan, S.D., Fälthammar, C.G., Block, L.P.: On the nature of large auroral zone electric fields at $1 - R_E$ altitude. J. Geophys. Res. **83**, 1049–1054, 1978

Stüdemann, W., Winterhoff, H.P.: Principle of operation, performance and first results of the energetic particle instruments onboard the Substorm- and Porcupine-payload. BMFT-Report, BMFT-FB-W., 1980 (in press)

Received May 16, 1980; Revised Version September 15, 1980
Accepted September 16, 1980